Proc. Natl. Acad. Sci. USA
Vol. 96, pp. 3017–3022, March 1999
Immunolgy

Lymphocyte function-associated antigen-1 binding residues in intercellular adhesion molecule-2 (ICAM-2) and the integrin binding surface in the ICAM subfamily

JOSÉ M. CASASNOVAS*, CRISTIANA PIERONI, AND TIMOTHY A. SPRINGER†

The Center for Blood Research and Harvard Medical School, Department of Pathology, 200 Longwood Avenue, Boston, MA 02115

Contributed by Timothy A. Springer, December 24, 1998

ABSTRACT **The crystal structure of intercellular adhesion molecule-2 (ICAM-2) revealed significant differences in the presentation of the critical acidic residue important for integrin binding between I and non-I-domain integrin ligands. Based on this crystal structure, we mutagenized ICAM-2 to localize the binding site for the integrin lymphocyte function-associated antigen-1 (LFA-1). The integrin binding site runs diagonally across the GFC β-sheet and includes residues on the CD edge of the β-sandwich. The site is oblong and runs along a flat ridge on the upper half of domain 1, which is proposed to dock to a groove in the I domain of LFA-1, with the critical Glu-37 residue ligating the Mg^{2+} in the I domain. Previous mutagenesis of ICAM-1 and ICAM-3, interpreted in light of the recently determined ICAM-1 and ICAM-2 structures, suggests similar binding sites. By contrast, major differences are seen with vascular cell adhesion molecule-1 (VCAM-1), which binds α_4 integrins that lack an I domain. The binding site on VCAM-1 includes the lower portion of domain 1 and the upper part of domain 2, whereas the LFA-1 binding site on ICAM is confined to the upper part of domain 1.**

Intercellular adhesion molecule-2 (ICAM-2) is a cell surface glycoprotein that is a ligand for the integrin lymphocyte function-associated antigen-1 (LFA-1) and is constitutively expressed on endothelium, platelets, lymphocytes, and monocytes (1, 2). The extracellular domain of ICAM-2 consists of two Ig superfamily (IgSF) domains. These are about 35% identical in sequence to the first two IgSF domains of ICAM-1, ICAM-3, ICAM-4, and ICAM-5, which also function as ligands for LFA-1 (1, 2). The ICAMs are more distantly related to mucosal addressin cell adhesion molecule-1 (MAdCAM-1) and vascular cell adhesion molecule-1 (VCAM-1), which bind α_4 integrins. All of these IgSF molecules are more closely related to one another than to other members of the IgSF and appear to constitute a subfamily that is specialized for binding to integrins. The IgSF integrin ligands play specific and in some cases overlapping roles in leukocyte recirculation and recruitment at sites of inflammation, antigen-specific T cell responses and other cell–cell interactions essential for immune surveillance (1).

Significant differences among the IgSF integrin ligands correlate with the types of integrins to which they bind. LFA-1 to which ICAMs bind contains an inserted or I domain in its α subunit (3). The crystal structure of the I domain in LFA-1 and the related Mac-1 (CD11b/CD18) integrin has been defined and contains a Mg^{2+} that is required for ligand binding (4, 5). This Mg^{2+} is surrounded by residues that are required for specific ligand recognition, and thus define a ligand-binding interface on the I domain (6). The ICAMs contain a conserved Glu residue in domain 1 that is critical for binding to LFA-1 (7); the Mg^{2+} in the I domain has been proposed to coordinate an acidic residue in integrin ligands (4). By contrast, VCAM-1 and MAdCAM-1 bind to the $\alpha_4\beta_1$ and $\alpha_4\beta_7$ integrins, which lack an I domain (1). Therefore, the binding site in the integrin must differ, and may involve both a β-propeller domain predicted in all integrin α subunits (8) and a domain with certain features resembling an I domain, including a Mg^{2+}-binding site, predicted in the integrin β-subunit (4, 9, 10).

Recently x-ray crystal structures for domains 1 and 2 of ICAM-2, ICAM-1, VCAM-1, and MAdCAM-1 have been solved (11–16). Although a conserved sequence bearing an integrin-binding L(I)-E(D)-T(S)-S(P)-L motif is present in all (17), it has markedly different architectures in ICAM-1 and ICAM-2 compared with VCAM-1 and MAdCAM-1. In VCAM-1 and MAdCAM-1, the critical Asp residue is highly exposed at the tip of a protruding loop built by the motif. In ICAM-2 and ICAM-1, the homologous Glu residue is present at the end of β-strand C and lies on a flatter surface on an edge of domain 1. To understand the molecular basis for recognition by integrins of cell adhesion molecules, it is important to map the recognition surfaces. Extensive mutagenesis studies on VCAM-1 have defined the binding footprint in the crystal structure for the integrins $\alpha_4\beta_1$ and $\alpha_4\beta_7$ (18, 19). Both residues in domain 1 and in domain 2 contribute to binding. Previously, mutations in ICAM-1 and ICAM-3 have been studied for their effects on binding to LFA-1, and a peptide has been identified in ICAM-2 that has binding activity for LFA-1 (7, 20–25). These studies have shown that mutations in ICAM-1 and ICAM-3 that affect binding to LFA-1 are localized to domain 1. The studies on ICAM-1 and ICAM-2 were carried out before their crystal structures were determined, and a structure for ICAM-3 is not yet available; therefore, both the design and interpretation of mutants and peptides have relied on models based on other IgSF domains.

The recent determination of the structure of ICAM-2 to 2.2 Å (11) has now enabled us to both design and interpret mutations in ICAM-2 based on its three-dimensional structure. The even more recent determination of the structure of ICAM-1 (12, 13), together with previous work on VCAM-1, enables comparisons of the integrin-binding footprints between ICAM-1 and ICAM-2 and between the ICAMs and VCAM-1.

MATERIALS AND METHODS

Plasmids and Mutagenesis. The complete ICAM-2 cDNA (26) was subcloned into the *Xba*I restriction site of pAprM9

The publication costs of this article were defrayed in part by page charge payment. This article must therefore be hereby marked "*advertisement*" in accordance with 18 U.S.C. §1734 solely to indicate this fact.

PNAS is available online at www.pnas.org.

Abbreviations: ICAM, intercellular adhesion molecule; LFA, lymphocyte function-associated antigen; VCAM, vascular cell adhesion molecule; IgSF, Ig superfamily; MAdCAM, mucosal addressin cell adhesion molecule.

*Present address: Center for Biotechnology, Department of Biosciences at Novum, Karolinska Institute, S-141 57 Huddinge, Sweden.
†To who reprint requests should be addressed. e-mail: springer@sprsgi.med.harvard.edu.

(23) to generate IC2/pAprM9. Mutagenesis was by the overlap PCR technique by using *Pfu*I polymerase (Stratagene) and IC2/pAprM9 as template, essentially as described (6). Mutations were identified by restriction analysis and confirmed by DNA sequencing.

Cell Transfection and LFA-1 Binding Assay. COS cells at 40–60% confluency in 100 mm Petri dishes were transfected by the DEAE-dextran method, resuspended by trypsin-EDTA treatment, and reseeded 1 day before the binding assay (7). Graded amounts of IC2/pAprM9 ranging from 0.1 to 8 μg and about 6 μg of mutant ICAM-2 cDNAs were used in each transfection. Three days after transfection cells were detached from the plates with 5 mM EDTA in PBS, washed two times with L15 medium/2.5% fetal calf serum (binding buffer), and resuspended in binding buffer at 2×10^6 cells/ml. Indirect immunofluorescence and flow cytometry was done with 50 μl of cell suspension for each anti-ICAM-2 mAb. The percentage of cells expressing ICAM-2 was determined after subtraction of background staining of cells mock-transfected with pAprM9.

For binding assays, immunopurified LFA-1 (27) (0.5 mg/ml) was diluted 100-fold with TSM buffer (20 mM Tris·HCl, 150 mM NaCl, 2 mM $MgCl_2$, pH 9.0), and 30 μl per well was applied to 96-well flat-bottom plates (Linbro) overnight at 4°C. Wells were blocked with 200 μl of 2% heat-treated BSA in binding buffer for 30 min at 37°C and washed two times with binding buffer before the assay. BCECF (Molecular Probes)-labeled cells (6) ($\approx 7 \times 10^4$) in 25 μl of binding buffer were added in triplicate to LFA-1-coated wells containing 75 μl of binding buffer. Cells were centrifuged at 1000 rpm for 1 min and incubated at 37°C for 30 min. Well-associated fluorescence was determined before and after removal of unbound cells by three to four gentle washes with 100 μl of binding buffer at room temperature, and the percentage of adherent cells was determined. The specific cell binding (%) was obtained by subtracting the background binding obtained with COS cells transfected with pAprM9.

RESULTS

By using the x-ray crystal structure of human ICAM-2 (11), we identified 25 residues in domain 1 that were surface exposed and were in the general vicinity of Glu-37, including some residues conserved in ICAM-1, ICAM-2, and ICAM-3. In domain 2, the two most well-exposed residues that are closest to E37 were selected for mutagenesis. These residues are in the C′E loop of domain 2. Residues were mutated to alanine, or in the case of Gly-35, to threonine. COS cells were transfected with varying amounts of wild-type ICAM-2 cDNA, and the percentage of cells expressing ICAM-2 and binding to purified LFA-1 was determined (Fig. 1*A*). This served as a standard curve for determination of LFA-1 binding activity and enabled correction for differences in surface expression between wild-type and mutant ICAM-2 constructs. COS cells transfected with ICAM-2 cDNA, but not with AprM9 vector, bound to purified LFA-1 immobilized on plastic (Fig. 1*B*). Binding was completely inhibited by mAb TS1/18 to LFA-1 and IC2/2 to ICAM-2. The ICAM-2 mAb BT-1 inhibited partially, and the ICAM-2 mAbs IC2/1 and 6D5 gave little or no inhibition. The lack of inhibition by 6D5 mAb may be related to the consistently lower amount of binding of this mAb to ICAM-2 found here by flow cytometry of transfected COS cells.

The mutations give a hint to where several of the mouse mAb bind to human ICAM-2 (Table 1). Definitive mapping would require extensive substitutions, because mouse and human ICAM-2 are only 54% identical in domain 1. Binding of mAb IC2/2 was affected by substitution of Q30 and E47 (Table 1), which are nearby one another in the upper portion of the CD edge of domain 1. The 6D5 mAb appears to recognize a partially overlapping epitope involving residues

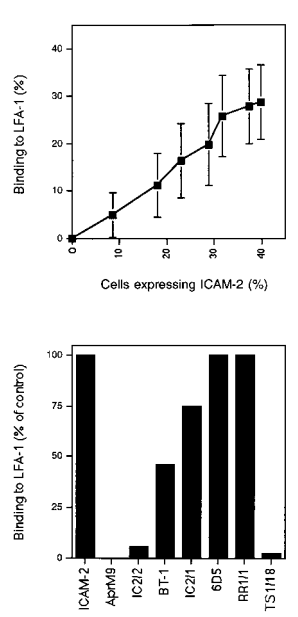

FIG. 1. Binding of COS cells expressing ICAM-2 to immobilized LFA-1 and effect of mAbs. (*A*) COS cells were transfected with 0, 0.1, 0.375, 0.75, 1.5, 3, 6, or 8 μg of ICAM-2 cDNA. The percentage of cells binding to purified LFA-1 adsorbed to plastic (*y*-axis) and expressing ICAM-2 by using the anti-ICAM-2 antibody CBR-IC2/1 and immunofluorescence flow cytometry (*x*-axis) was determined. Data are average and standard deviation for 10 different experiments. (*B*) Binding to LFA-1 of COS cells transfected with ICAM-2 or mock transfected with AprM9 was determined in the presence of 10 μg/ml of anti-ICAM-2 antibodies CBR-IC2/1, CBR-IC2/2, BT-1, and 6D5, anti-ICAM-1 mAb RR1/1, and LFA-1 β-subunit mAb TS1/18, respectively. The amount of binding to LFA-1 is expressed as a percentage of the binding obtained in the absence of mAb. Data are for an average of two to five experiments.

E47 and Q48. The 6D5 mAb binds less well than the other mAb to wild-type ICAM-2 and shows enhanced binding to several mutants. The 6D5 mAb was raised to ICAM-2 produced in *Escherichia coli* (28); mutants with increased 6D5 mAb binding may resemble the conformation of ICAM-2 that lacks N-linked glycosylation. None of the mutations selectively affected binding of IC2/1 mAb. The IC2/1 mAb does not inhibit binding of ICAM-2 to LFA-1, which suggests that it does not bind to the LFA-1 binding interface, consistent with the lack of effect of the mutations around E37 studied here.

To determine whether mutations were likely to widely disrupt ICAM-2 structure, they were examined for an effect on binding of all four mAbs, and for effect on solvent accessible surface area and hydrogen bonds (Table 1). The Y54/A mutation markedly reduced binding of all four mAbs; the K52/A substitution also affected binding of all four mAbs, but less severely. Solvent accessible surface area was determined by using the program DSSP (29) with the native structure, and with mutated residues truncated at Cβ to represent the alanine substitutions. Mutation of residues with side chains that are largely buried distal to Cβ yields an increase in accessible surface, and for those that are largely exposed yields a decrease. Mutation of residues Y54 and K52 gave the largest and third largest increase in solvent accessible area, consistent with destabilization (Table 1). Furthermore, mutation results in a loss of hydrogen bonds from the side chains of these residues to the main chains of residues L36 and G34, respectively. K42 also donates a hydrogen bond to L36; it is not possible to determine whether the low binding of mutant K42A to LFA-1 results from a specific effect or an overall effect on domain structure. The amount of binding to LFA-1 has been corrected for the amount of surface expression of mutants, and

Table 1. Binding of ICAM-2 mutants to LFA-1 and ICAM-2 antibodies

Mutant	Binding to LFA-1*	Binding to mAb†				Change in accessible surface, Å^2	Side chain H bonds
		IC2/1	IC2/2	BT-1	6D5		
ICAM-2	100	100	100	100	100	0	
Q30/A	107.9 ± 31	101 ± 3	44 ± 18	ND	130 ± 29	−63	
V33/A	**48.3 ± 11**	126 ± 12	115 ± 13	ND	96 ± 44	−8	
G35/T	**2.3 ± 1**	82 ± 6	78 ± 4	72 ± 4	117 ± 23	ND	
E37/A	**1.3 ± 2**	85 ± 16	83 ± 19	ND	86 ± 25	−2	
L40/A	**61.0 ± 23**	95 ± 24	93 ± 20	104 ± 31	65 ± 35	40	
N41/A	**57.6 ± 20**	108 ± 33	103 ± 27	112 ± 31	82 ± 33	−53	
K42/A	**10.3 ± 14**	62 ± 26	53 ± 27	ND	85 ± 48	15	L36 O
I43/A	94.0 ± 5	95 ± 7	94 ± 11	92 ± 11	156 ± 37	−25	
L44/A	3.6 ± 3	39 ± 14	12 ± 2	ND	163 ± 100	10	
L45/A	1.2 ± 1	32 ± 18	18 ± 14	11 ± 8	62 ± 20	21	
E47/A	84.0 ± 7	79 ± 19	6 ± 3	ND	27 ± 18	−20	
Q48/A	103.6 ± 13	86 ± 14	64 ± 15	82 ± 2	34	−57	
Q50/A	107.6 ± 18	86 ± 25	83 ± 22	ND	168 ± 100	−3	N29 OD1
K52/A	13.5 ± 12	50 ± 6	31 ± 3	39 ± 2	51 ± 20	47	G34 O
Y54/A	4.4 ± 3	31 ± 1	5 ± 4	0	5 ± 6	70	L36 N
L55/A	98.2 ± 20	54 ± 4	64 ± 8	50 ± 16	40	−21	
S57/A	114.3 ± 26	75 ± 22	67 ± 25	77 ± 20	78 ± 44	14	
S60/A	139.3 ± 32	65 ± 18	56 ± 24	64 ± 14	74 ± 24	−12	
D62/A	100.2 ± 13	53 ± 16	41 ± 21	49 ± 7	78	−31	V84 N, R175 NH1
Q66/A	80.4 ± 24	99 ± 21	92 ± 18	97 ± 22	105 ± 59	1	
H68/A	**0 ± 0**	82 ± 25	76 ± 29	ND	151 ± 68	51	
T70/A	**13.4 ± 9**	71 ± 26	64 ± 25	58 ± 15	126 ± 26	17	
Q75/A	**2.0 ± 2**	88 ± 12	84 ± 32	72 ± 42	113 ± 20	6	
S77/A	104.0 ± 18	82 ± 10	85 ± 9	66 ± 6	76	6	
N79/A	93.2 ± 6	124 ± 50	119 ± 36	114 ± 45	130 ± 100	−13	L65 O
Q145/A	103.1 ± 3	105 ± 21	102 ± 16	97 ± 12	97 ± 42	1	
E146/A	93.0 ± 14	74 ± 1	73 ± 0	88 ± 18	41 ± 12	−13	T114 N

*Binding to LFA-1 of ICAM-2 mutants (average ± SD for three experiments) was normalized to the amount of mutant ICAM-2 expression using a standard curve like that shown in Fig. *1A* in each experiment. ICAM-2 expression was determined with CBR/IC2/1 mAb, except for three mutants with lowered binding of IC2/1 mAb, which were normalized with IC2/2 mAb.

†Binding of mAb to mutants was normalized to the percentage of wild-type transfectants stained with the same mAb (average ± SD for three experiments, with some single determinations). The percentage of wild-type transfectants stained with IC2/1, IC2/2, BT-1, and 6D5 mAb averaged 37 ± 16%, 38 ± 16%, 34 ± 13%, and 9 ± 6%, respectively (average ± SD for 14 experiments). Residue numbering is revised based on recent determination of the beginning of the mature ICAM-2 sequence (11).

it should be pointed out that L55A, S60A, and D62A show a decrease in surface expression measured with all four mAbs, similar to that of K42A, yet their binding to LFA-1 is unaffected (Table 1).

The LFA-1 binding interface on ICAM-2 includes the upper part of the GFC face and the CD edge of domain 1 (Figs. 2 and 3*A*). A two log decrease in binding to LFA-1 was seen after mutation of G35 and E37 in strand C, H68 in strand F, and Q75 in strand G (Table 1). Mutation of residues V33 and T70, which are higher in strands C and F, respectively, diminished binding 8- and 2-fold, respectively. K42 appears to form part of the LFA-1 binding interface, but the hydrogen bond donated by its side chain to the carbonyl O of L36 (Fig. 3*A*) could also have a role in orienting the side chain of E37. A homologous hydrogen bond is found in ICAM-1 (Fig. 3*B*), and this lysine is conserved in all ICAMs (Fig. 2), suggesting that this is an important side chain—main chain hydrogen bond (30). Residues L40 and N41 in the CD loop appears to make a specific but modest contribution to binding LFA-1. The L44A and L45A mutations greatly diminished LFA-1 binding, but also affected binding of multiple mAb (Table 1). It is interesting that all four residues that affected binding of both LFA-1 and multiple mAbs, L44, L45, K52, and Y54, clustered nearby one another on strands D and E (see Fig. 3A). Mutation of 12 other residues adjacent to those described above had no effect and showed that the binding surface for LFA-1 was highly circumscribed (see Fig. 3 and Table 1). Mutations of nearby residues in domain 2, Q145 and E146, also were without effect (Table 1).

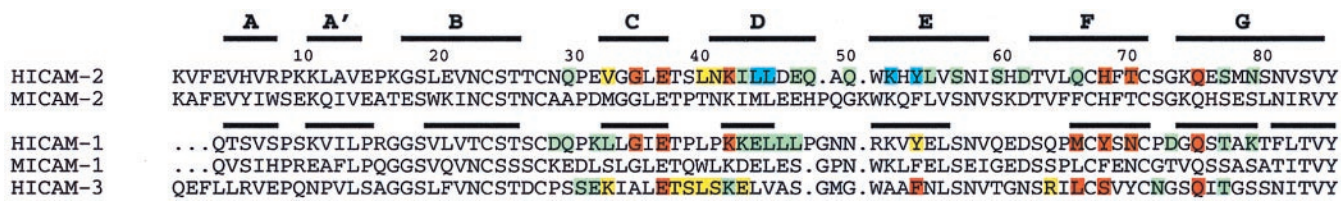

FIG. 2. LFA-1 binding residues in the ICAM subfamily of adhesion receptors. N-terminal domains of ICAM-1 and -2 were structurally aligned with 3DMALIGN of MODELLER with a gap penalty of 1.75 Å (12), and ICAM-3 was aligned based on sequence homology. Thick lines represent β-strands in the structures of ICAM-2 and ICAM-1. Residues found important for LFA-1 recognition by single residue mutagenesis experiments as described here for ICAM-2 or elsewhere for ICAM-1 or ICAM-3 (7, 20–23, 25) are color-coded according to percentage of wild-type binding: red, severe, <35%; orange, moderate, 35–70%; green, little or no effect, 70–100%; cyan, <35% binding with a possible effect of the mutation on structural integrity. Mutation was to alanine, except for mutations Y52/F (7) and Y66/S (20) in ICAM-1, G35/T in ICAM-2, and mutations L66/K and S68/K in ICAM-3 (21).

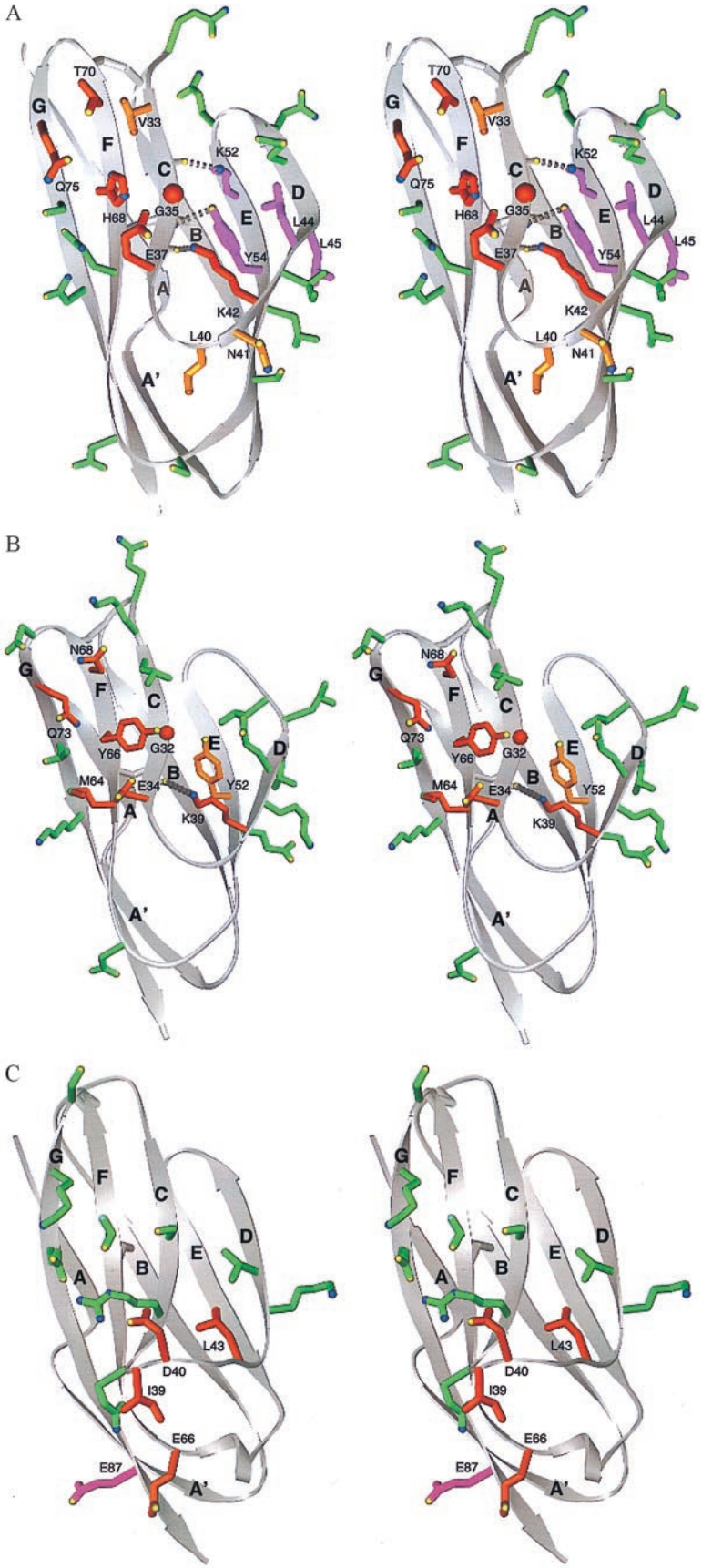

FIG. 3. Integrin binding surfaces in the crystal structures of domain 1 of ICAM-2, ICAM-1, and VCAM-1. Stereoviews are of ICAM-2 (*A*), ICAM-1 (*B*), and VCAM-1 (*C*). The backbone is shown in grey as a ribbon diagram (34) with β-strands lettered. Disulfide bonds are shown in gray. Side chains of individual residues tested by mutagenesis are shown as ball and stick. The carbons and bonds of these side chains are color-coded according to the percentage of wild-type binding to LFA-1 after mutagenesis (see Table 1 and Fig. 2 legend): red, <35%; yellow-orange, 35–70%; green, >70%; magenta, <35% with a possible effect on domain structure. Side chain oxygen and nitrogen atoms are yellow and blue, respectively.

DISCUSSION

Our results define the binding site for LFA-1 on ICAM-2 within the context of its crystal structure (11). This surface extends diagonally across the GFC face and CD edge of domain 1 (see Fig. 3*A*). Residues showing the greatest specific effect on binding, and that may therefore be central in the binding site, are Q75 at the top of strand G, T70 and H68 at the top of strand F, G35 and E37 at the bottom of strand C, and K42 at the bottom of strand D. Residues Y54, K52, L44, and L45 may contribute directly or indirectly to binding of LFA-1. Mutation of V33, L40, and N41 has a lesser effect on binding. This finding suggests that they are located on the periphery of the binding site, in agreement with their position peripheral to the more important residues in the crystal structure. The side chain of L40 is buried, and therefore the modest effect of mutation of this residue may result from a change in packing around the CD loop. Finally, 12 residues with little or no effect on binding surround the above binding site. The shape of the binding site is strikingly oblong; the six most important residues defined here describe a surface approximately 15 Å long and 5 Å wide. Inclusion of the three less important residues defines a larger oblong surface, $\approx 25 \times 7$ Å, and inclusion of residues with either a direct or indirect effect on binding defines a surface $\approx 25 \times 10$ Å.

The recent crystal structures for ICAM-1 (12, 13) enable previous mutagenesis studies on ICAM-1 and ICAM-3 (7, 20–23, 25) to be interpreted at atomic level. The binding surfaces show marked similarity, with the differences confined to residues on the periphery of the binding sites (Figs. 2 and 3). Four positions corresponding to E37, Y54, H68, and Q75 in ICAM-2 are important in all three ICAMs (Fig. 2). Two of these, E37 and Q75, are conserved in ICAM-1, -2, and -3, and all four residues are nearby one another (Fig. 3*A* and *B*). These results suggest that ICAM-1, -2, and -3 bind in similar orientations to LFA-1.

It is interesting that the key LFA-1 binding residues are hydrophilic; this is unusual for protein–protein interactions, but is also observed for the interaction of CD2 with LFA-3 (31). The key Glu-37 residue has been suggested to be responsible for the Mg^{2+} ion dependence of the LFA-1 interaction with ICAM-1 (7, 32), and to coordinate with a Mg^{2+} in the I domain of LFA-1 (4). The side chains of Glu-37 and Gln-75 in ICAM-2 point toward one another, placing their polar groups in close proximity (Fig. 3*A*), as also seen for the equivalent Glu-34 and Glu-73 residues in ICAM-1 (Fig. 3*B*). Only modest side chain rotations would be required to obtain orientations for the polar atoms of E37 and Q75 in ICAM-2 and their homologues in ICAM-1 that would be structurally equivalent, and thus to obtain nearly identical polar interactions with LFA-1.

Although domains 1 and 2 of ICAM-1, ICAM-2, and VCAM-1 are structurally homologous, the integrin binding footprint of VCAM-1 differs markedly (Fig. 3*C*). The different conformations around the critical Glu residue in ICAMs and Asp residue in VCAM-1 and MAdCAM-1 (30) have already been remarked. The Asp is in a protruding loop, whereas the Glu is in a β-strand and is in a relatively flat surface. Our results emphasize additional marked differences between ICAMs and VCAM-1 in the location of the integrin binding face. Although Glu-37 in ICAM-2 and Asp-40 in VCAM-1 both lie approximately in the middle of domain 1, most of the other important integrin binding residues are in the upper half of domain 1 in ICAM-2 (Fig. 3*A*), and in the lower half of domain 1 in VCAM-1 (Fig. 3*C*) (18, 19, 33). Coinciding with this distinct localization of the binding sites in domain 1, important residues in ICAMs tend to be in β-strands whereas those in VCAM-1 tend to be in loops. Furthermore, domain 2 contributes to integrin binding in VCAM-1 but not in ICAM-2. The lack of a contribution by domain 2 in ICAMs is confirmed for ICAM-3, in which domain 1 can be expressed without domain 2 and binds equally as well as intact ICAM-3 (23).

The oblong LFA-1 binding surface on ICAM-2 and ICAM-1 is present on a long, flat ridge in domain 1 (Fig. 3 *A* and *B*) and has a geometry appropriate for docking into a groove in the I domain. Interestingly, four residues responsible for species specific interactions between ICAM-1 and LFA-1 map to a groove 25 Å long in the I domain, that runs through the Mg^{2+} ion-dependent adhesion site (MIDAS) (5, 6). We propose that the ridge we have defined in ICAM-2 docks to the groove in the LFA-1 I domain, with coordination of Glu-37 to the Mg^{2+} near the center of an oblong, ridge-groove complementary binding site.

We thank Dr. Chafen Lu for purified LFA-1 and Dr. Chichi Huang for technical advice. This work was supported by National Institutes of Health Grant CA31798.

1. Springer, T. A. (1994) *Cell* **76,** 301–314.
2. Dustin, M. L. & Springer, T. A. (1999) in *Guidebook to the Extracellular Matrix and Adhesion Proteins,* eds. Kreis, T. & Vale, R. (Sambrook & Tooze, New York).
3. Larson, R. S., Corbi, A. L., Berman, L. & Springer, T. A. (1989) *J. Cell Biol.* **108,** 703–712.
4. Lee, J-O., Rieu, P., Arnaout, M. A. & Liddington, R. (1995) *Cell* **80,** 631–638.
5. Qu, A. & Leahy, D. J. (1995) *Proc. Natl. Acad. Sci. USA* **92,** 10277–10281.
6. Huang, C. & Springer, T. A. (1995) *J. Biol. Chem.* **270,** 19008–19016.
7. Staunton, D. E., Dustin, M. L., Erickson, H. P. & Springer, T. A. (1990) *Cell* **61,** 243–254.
8. Springer, T. A. (1997) *Proc. Natl. Acad. Sci. USA* **94,** 65–72.
9. Tozer, E. C., Liddington, R. C., Sutcliffe, M. J., Smeeton, A. H. & Loftus, J. C. (1996) *J. Biol. Chem.* **271,** 21978–21984.
10. Tuckwell, D. S. & Humphries, M. J. (1997) *FEBS Lett.* **400,** 297–303.
11. Casasnovas, J. M., Springer, T. A., Liu, J.-h., Harrison, S. C. & Wang, J.-h. (1997) *Nature (London)* **387,** 312–315.
12. Casasnovas, J. M., Stehle, T., Liu, J.-h., Wang, J.-h. & Springer, T. A. (1998) *Proc. Natl. Acad. Sci. USA* **95,** 4134–4139.
13. Bella, J., Kolatkar, P. R., Marlor, C., Greve, J. M. & Rossmann, M. G. (1998) *Proc. Natl. Acad. Sci. USA* **95,** 4140–4145.
14. Jones, E. Y., Harlos, K., Bottomley, M. J., Robinson, R. C., Driscoll, P. C., Edwards, R. M., Clements, J. M., Dudgeon, T. J. & Stuart, D. I. (1995) *Nature (London)* **373,** 539–544.
15. Wang, J.-h., Pepinsky, R. B., Stehle, T., Liu, J.-h., Karpusas, M., Browning, B. & Osborn, L. (1995) *Proc. Natl. Acad. Sci. USA* **92,** 5714–5718.
16. Tan, K., Casasnovas, J. M., Liu, J.-h., Briskin, M. J., Springer, T. A. & Wang, J.-h. (1998) *Structure (London)* **6,** 793–801.
17. Vonderheide, R. H., Tedder, T. F., Springer, T. A. & Staunton, D. E. (1994) *J. Cell Biol.* **125,** 215–222.
18. Kilger, G., Clements, J. & Holzmann, B. (1997) *Int. Immunol.* **9,** 219–226.
19. Newham, P., Craig, S. E., Seddon, G. N., Schofield, N. R., Rees, A., Edwards, R. M., Jones, E. Y. & Humphries, M. J. (1997) *J. Biol. Chem.* **272,** 19429–19440.
20. Fisher, K. L., Lu, J., Riddle, L., Kim, K. J., Presta, L. G. & Bodary, S. C. (1997) *Mol. Biol. Cell* **8,** 501–515.
21. Holness, C. L., Bates, P. A., Littler, A. J., Buckley, C. D., McDowall, A., Bossy, D., Hogg, N. & Simmons, D. L. (1995) *J. Biol. Chem.* **270,** 877–884.
22. Sadhu, C., Lipsky, B., Erickson, H. P., Hayflick, J., Dick, K. O., Gallatin, W. M. & Staunton, D. E. (1994) *Cell Adhes. Commun.* **2,** 429–440.
23. Klickstein, L. B., York, M. B., de Fougerolles, A. R. & Springer, T. A. (1996) *J. Biol. Chem.* **271,** 23920–23927.
24. Li, R., Nortamo, P., Valmu, L., Tolvanen, M., Huuskonen, J., Kantor, C. & Gahmberg, C. G. (1993) *J. Biol. Chem.* **268,** 17513–17518.
25. Bell, E. D., May, A. P. & Simmons, D. L. (1998) *J. Immunol.* **161,** 1363–1370.

26. Staunton, D. E., Dustin, M. L. & Springer, T. A. (1989) *Nature (London)* **339,** 61–64.
27. Dustin, M. L., Carpen, O. & Springer, T. A. (1992) *J. Immunol.* **148,** 2654–2663.
28. Nortamo, P., Salcedo, R., Timonen, T., Patarroyo, M. & Gahmberg, C. G. (1991) *J. Immunol.* **146,** 2530–2535.
29. Kabsch, W. & Sander, C. (1983) *Biopolymers* **22,** 2577–2637.
30. Wang, J.-h. & Springer, T. A. (1998) *Immunol. Rev.* **163,** 197–215.
31. Davis, S. J., Ikemizu, S., Wild, M. K. & van der Merwe, P. A. (1998) *Immunol. Rev.* **163,** 217–236.
32. Marlin, S. D. & Springer, T. A. (1987) *Cell* **51,** 813–819.
33. Chiu, H. H., Crowe, D. T., Renz, M. E., Presta, L. G., Jones, S., Weissman, I. L. & Fong, S. (1995) *J. Immunol.* **155,** 5257–5267.
34. Carson, M. (1987) *J. Mol. Graph.* **5,** 103–106.